DOI: 10.1784/ndt2025.2b1

Use of CIVA to determine optimal settings for the inspection of bonded 1.6 mm aluminium plates with thermography

H. Patrick Jansen and Daniella B. Deutz
Royal Netherlands Aerospace Centre,
Marknesse, 8316 PR, The Netherlands
+31 88 511 43 33
patrick.jansen@nlr.nl

Abstract

In the pursuit of efficient Non-Destructive Testing (NDT) techniques for inspecting adhesively bonded metals, thermography has emerged as a promising approach. This study leverages the thermography module from the Extende CIVA software to optimize inspection settings for two 1.6 mm aluminium plates which are adhesively joined together. The research focuses on comparing various excitation techniques, including Flash, long pulsed thermography and lock-in thermography, both in single-sided and through-transmission inspection modes.

The objective is to evaluate the effectiveness of these techniques in detecting defects such as porosity, inserts, and debonds in adhesively bonded metallic structures. Simulated results are compared to experiments to ensure accuracy and reliability. By analysing the outcomes of different thermography techniques, this study aims to identify the most efficient and accurate approach for inspecting adhesively bonded metallic structures.

The findings of this research have significant implications for the development of fast and reliable NDT techniques in the aerospace and automotive industries, where adhesively bonded metals are widely used.

Introduction

Aluminium bonded panels are commonly used in aircraft structures. In general, the lay-up consists of aluminium panels with varying thickness bonded with an adhesive. To ensure the integrity of newly produced panels, typically an ultrasonic inspection is performed by transmitting ultrasound through the panel. However, there are some drawbacks using this approach like the need for couplant, and slow scanning times. In this work, active thermography is investigated as a potential technique for inspection both in simulations as well as experiment.

Materials and methods

Reference panels

Reference specimens were supplied by GKN Fokker Aerospace. Three types of panels were made consisting of two 400x400x1.6 mm^3 aluminium sheets (AA 2024 – T3 AL clad) that are bonded together using 3M Scotch-3 Weld structural adhesive film

AF163-2K.06WT, with a nominal thickness of 0.15 mm. One panel contains inserts, one panel contains contamination (resulting in a debond) and one panel contains porosity. Figure 1 shows through transmission ultrasonic results at 5 MHz, showing the details of the panels. More details of the TT measurements are published elsewhere[1].

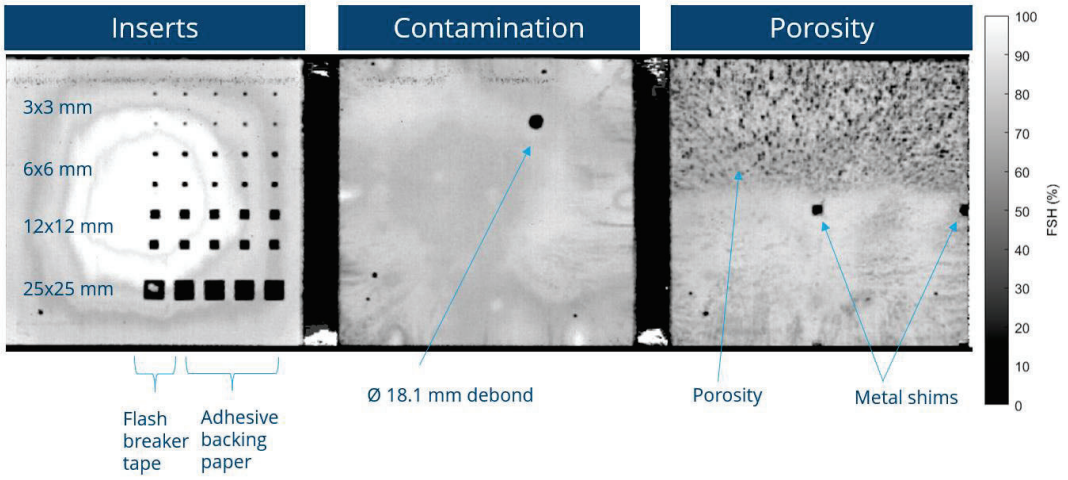

Figure 1: Through transmission ultrasonic C-scan results at 5 MHz showing the three different types of panels that have been supplied.

Simulations

Using the software package Civa from Extende simulations for thermography can be performed. This is a recently (start 2022) developed package inside of Civa which is mainly used for ultrasonic and x-ray simulations. In simulation, heat transfer is modelled in a single direction in plane and out of plane in the sample.

Figure 2 shows an overview of the defect that has been modelled. Two pieces of aluminium with a thickness of 1.6 mm have been modelled with an epoxy layer of 0.25 mm in between the aluminium sheets. For all simulations performed, a single defect with a lateral size of 30x30 mm is considered. The defect has a thickness of 0.25 mm, so the absence of the entire bond layer at this location has been modelled. The thermal properties used for all materials are indicated in Table 1. For the defect the thermal properties of air are taken, simulating a debond. During simulations, the low emissivity of the bare aluminium is not taken into account and is set to 1.

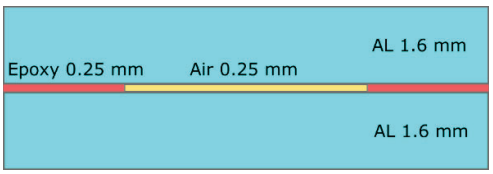

Figure 2: Schematic cross-sectional overview of the modelled defect.

The infrared camera is modelled as a perfect detector containing no noise, such that even the sightliest change in temperature can be detected. This is not the case for the

experiments were the camera has a noise equivalent temperature difference (NETD) of 25 mK.

Table 1: Thermal properties used for the CIVA simulations.

Material	Thermal conductivity (W / m K)	Heat Capacity (J / K m^3)
Aluminium	237	2.3976 * 10^6
Epoxy	0.63	1.5 * 10^6
Air	0.026	1313

In total 6 different experimental situations are considered, Flash, Long pulse, and lock-in thermography, both in single sided (SS) and through transmission (TT). Each different excitation method will be discussed in a separate section.

Flash thermography

Flash thermography uses a high powered flash light to heat up the surface. The duration of the flash is very short (~1/20s) giving an impulse response to the component investigated. The amplitude, given in J/m^2 can be varied in experiment by using less charge on the lamps, or by positioning the lamps further away. The energy density has been varied for the simulations for both the SS and TT inspection.

Figure 3 shows the resulting temperature vs time plots for the single sided flash and the through transmission flash. There is a difference in temperature as a function of time between sound and defect area. In a SS inspection, the material heats up due to the flash, whenever there is a defect present (dashed line) the cooldown with respect to sound material is slower due to the hindered heat transport of the defect. In TT mode, this is the other way around. Here the defects also hinders transport, resulting in lower surface temperatures. Temperature increases as the energy density becomes larger.

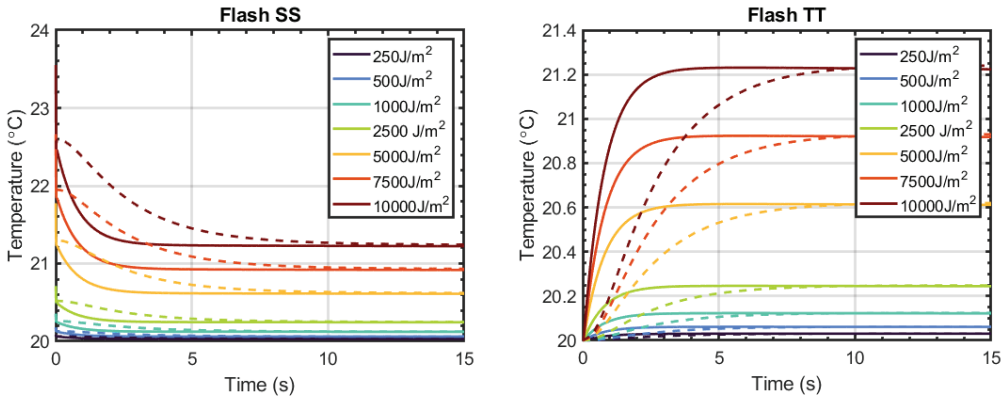

Figure 3: (left) Temperature vs time for different energies for flash thermography in single sided mode. (right) Temperature vs time for different energies for flash thermography in through transmission mode.

To better see the effects of the different energy densities, ΔT between the defect and sound area is plotted in Figure 4. For both SS and TT, the magnitude of ΔT becomes larger as the energy density is increased. The maximum magnitude is reached in a single sided inspection. For both SS and TT the ΔT is close to 0 after 10 s, indicating that detection of the defect should happen on short time scales.

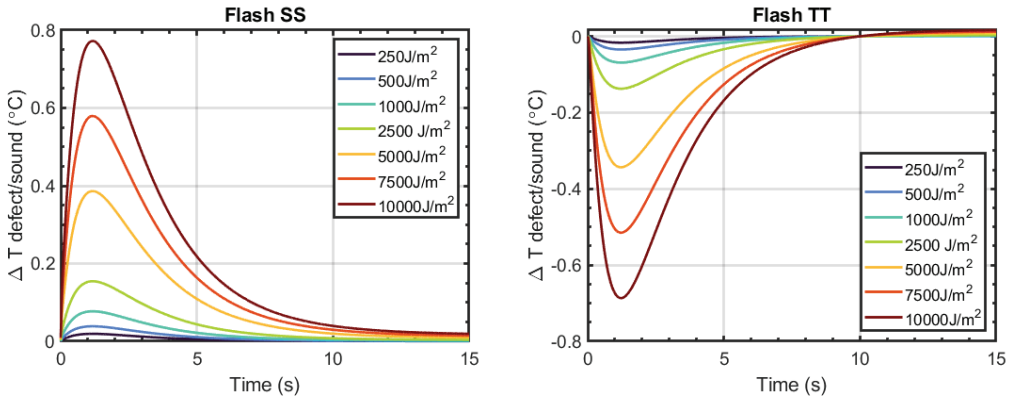

Figure 4: Difference in temperature between sound material and defect material as a function of time. (left) in single sided inspection. (right) in through transmission inspection.

Concluding, flash can be used to detect defects, as long as sufficient energy densities can be reached. If the energy density is too low the resulting temperature difference is too small to enable detection of a defect.

Long pulsed thermography

For long pulsed thermography, a pulse with a certain length is applied using halogen lamps and the time transient is recorded.. The benefit is that more energy can be supplied to the test subject as compared to the flash excitation. The pulse duration and the amount of energy can be changed. First, the effect of pulse length is investigated at a fixed energy density of 500W/m^2. Figure 5 shows the temperature vs time plots with varying pulse length for SS and TT inspections.

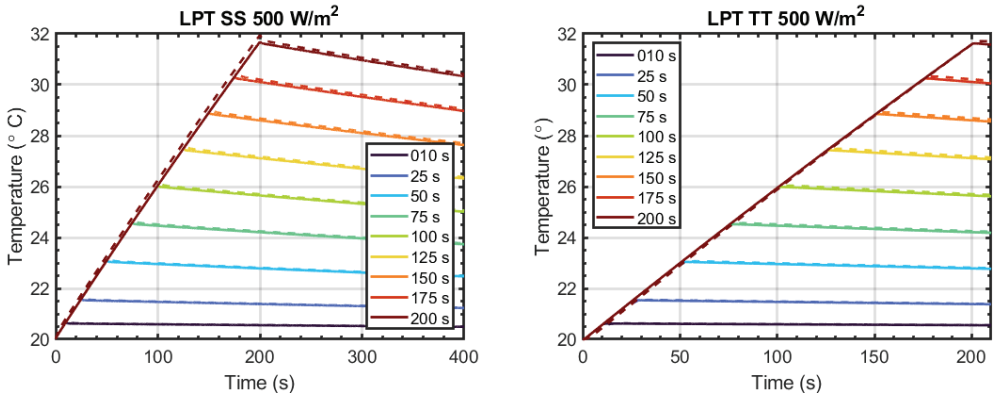

Figure 5: Temperature vs time for LPT simulations with variation in pulse length. The solid line is on sound material, and the dashed lines are on the defect. (left) For a single sided inspection and (right) for a through transmission.

Pulse length has been varied between 10 seconds, and 200s and the total time of recording for a SS inspection is 400 seconds, while for the TT it is 210 seconds. The solid lines, are the temperature readings on sound material and the dashed lines are on the defect. With increasing pulse length the overall temperature that is reached becomes higher. The area above the defects heats up slightly faster as compared to the sound material for the SS inspection. Once the pulse has finished, the sample starts to cool with the defect surface temperature slightly lagging behind of the sound material surface temperature. For the TT measurement the temperature above a defect slightly lags behind the sound material. During cooldown there is a slight difference between the defect area and the sound area. In order to get a better grip on the temperature difference ΔT is plotted as a function of time. Figure 6 shows the temperature difference between the sound material and the defect material as a function of time.

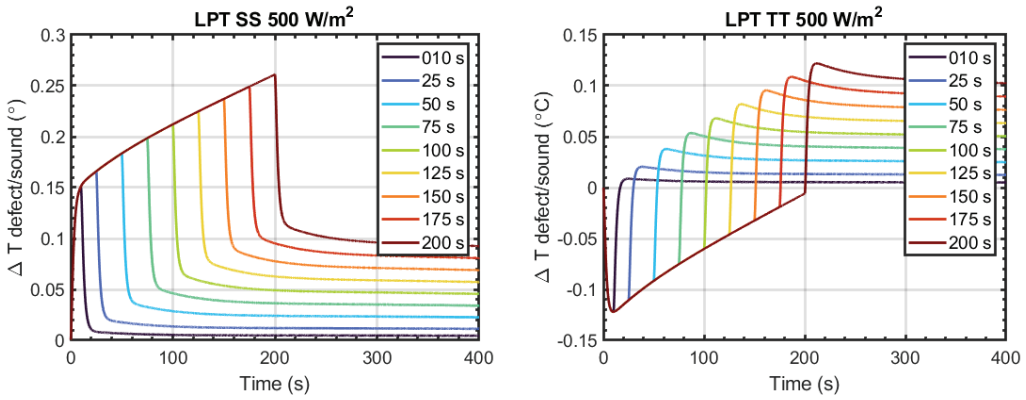

Figure 6: Difference in temperature between the sound material and the defect material as a function of time. (left) for a single sided inspection and (right) for a through transmission.

For a SS inspection, as the pulse length is increased the difference between the sound area and the defect area is maximum at the end of the pulse. Subsequently, as the surface starts

to cooldown this difference decreases again. However, the sharpest increase seems to happen in the first 10 seconds. For the TT case, the magnitude of ΔT decreases with longer pulse lengths. Once, the pulse is done the temperature difference becomes positive due to less cooldown due to the defect. For both SS and TT simulations, the absolute temperature difference between the defect and the sound material is quite low. Increasing the pulse length by a factor of 20 results in a ΔT of less than a factor of 2 for SS and for TT increasing the pulse length leads to a decrease in ΔT. Indicating, that the pulse length is not an essential variable (as long as sufficient time has been reached).

An increase in power density is also simulated. This has been done for a pulse length of 20 seconds. The results are shown in Figure 7 where ΔT is plotted as a function of time for both the SS and TT inspection. As the power is increased ΔT increases for the SS inspection. For the TT inspection the defect has a lower temperature as compared to sound material, but this difference also increases with higher power densities. The maximum temperature difference increases as the amount of power is increased. At about 10 seconds, a plateau is reached meaning that increasing the pulse length does not increase ΔT significantly.

For experiments, it is therefore crucial to apply as much power in the 10 seconds in order to see temperature differences on the surface. However, it should be noted that the maximum temperature reached at a power density of 10 kW/m^2 is around 45 °C which is already quite high.

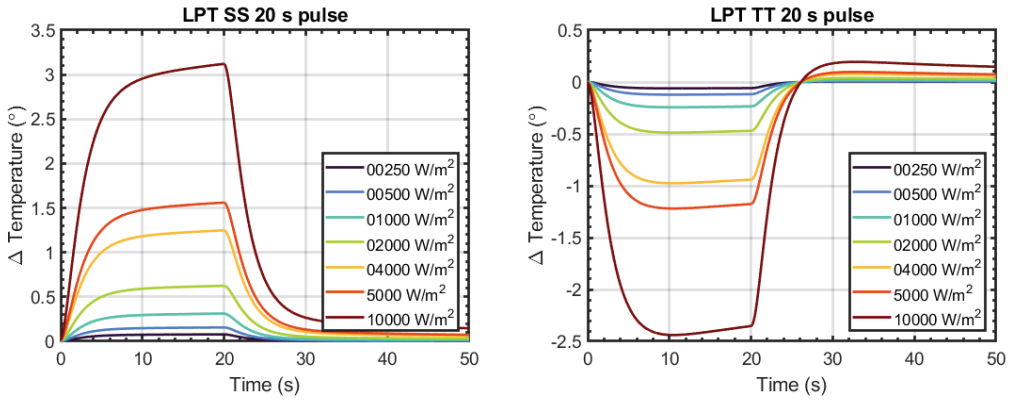

Figure 7: ΔT vs time curve for a 20 second pulse at different power settings for excitation. (left) single-sided inspection (right) through transmission.

Concluding for an LPT measurement, increasing pulse length does not improve contrast, only using higher energy densities does.

Lock-in thermography

Lock-in thermography uses halogen lamps to heat up the surface. The modulation that is used on the lamps has a sinusoidal shape of which the amplitude and frequency can be set. A predetermined number of periods can be recorded, with the benefit that the noise

in the measurement decreases as more periods are recorded. First, the effect of the lamp frequency is investigated for three power densities. The frequency of excitation is set, going from 0.001 until 100 Hz in 21 steps. The amplitude is varied in three steps, 500, 2500 and 5000W/m^2. The simulation time is set such that 10 acquisition cycles are captured for all frequencies. From these simulations the amplitude and phase difference of the defect with respect to sound material is extracted. Figure 8 shows this amplitude and phase difference as function of frequency, for both a SS as TT simulation.

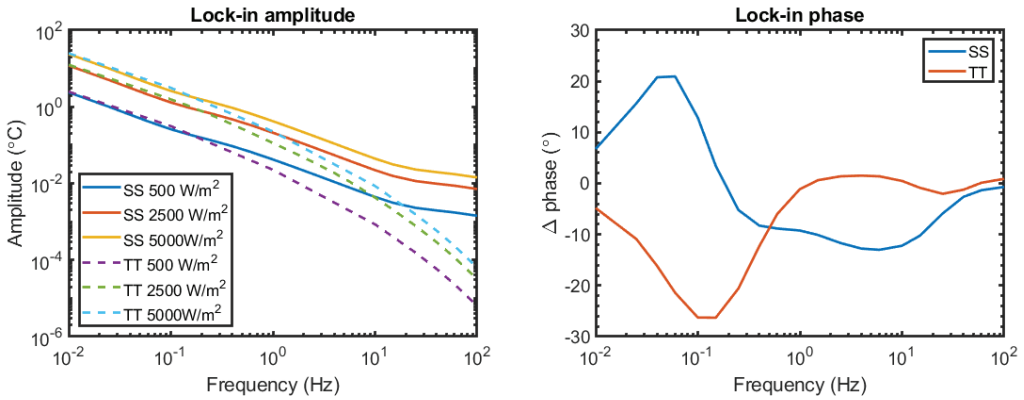

Figure 8: (left) Amplitude vs frequencies for different energies. (right) Delta phase vs frequency for optical lock-in thermography.

If the phase difference is 0, the defect cannot be detected. The difference in phase, is independent of the amplitude that has been used for excitation, resulting in a single graph for the single sided and through transmission, respectively. Normally, the best frequency for inspection is the highest frequency at which the difference in phase has the most negative value. In the case for the single sided inspection this is at 6 Hz and for TT this is at 0.15 Hz. From the amplitude data, we can see that for a single sided inspection no signal is expected at 6 Hz (due to the low amplitude), and therefore the defect cannot be measured in practice. While, in the case of a TT inspection this minimum is at lower frequencies, which can be measured using lock-in thermography.

Experiments

Using the knowledge gained from simulations, experiments have been performed but not for all situations considered in the simulations. The flash lamp used for experiments has a total output power of 4000J. In the case of a SS inspection the flash lamp cannot be put close enough to the surface, leading to very low energy densities resulting in a ΔT that is too low to be measured. For SS lock-in inspections the frequency at which a defect has the highest contrast is 6 Hz. However, at 6 Hz the amplitude of the signal is too low to be measured. Two types of excitation remain, Flash in TT mode and Lock-in in TT mode.

Flash TT

Flash in TT mode has been performed experimentally on the panel containing a debond. The flash lamp (max 6000J) was positioned as close to the sample as possible, illuminating an area of 188 x 188 mm^2, leading to high power densities of 170 kJ/m^2. An infrared camera (imgir40, 640x512, MWIR) was used to record the heat-up of the sample. Figure 9 shows the results of the experiment, where a single pixel value is plotted against time for a location containing a defect and a sound location for reference. Due to non-uniformities in the background the first frame is subtracted from the data such that the heat-up of the sample is better visualized. The total heat-up of the sample is quite low with about max 0.4 °C when compared to simulations. However, in the simulations the emissivity was not taken into account while the actual sample has an ε≈0.16 leading to much lower values read by the camera. On a piece of high ε tape the temperature increase was 2.77 °C.

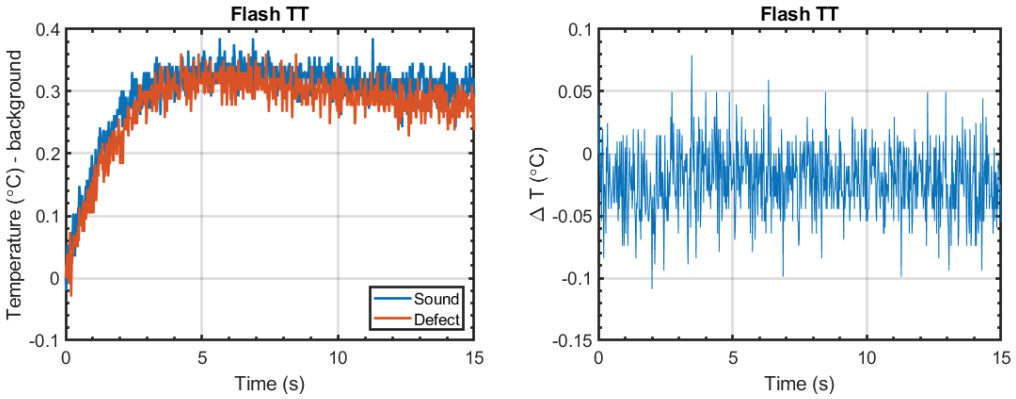

Figure 9: Flash TT experiment. (left) Temperature vs time with a background subtraction. (Right) ΔT between defect and sound material as a function of time.

The difference between the sound and defect is very low making it impossible to separate the defect from the sound material. To get a better signal from the IR camera the sample was coated with white developer, increasing ε to 0.3. Figure 10 shows the result by repeating the experiment where the sample has in increase in emissivity. In this case, more difference can be seen between the sound and defect material, where the defect material remains colder as compared to the sound material. The simulations with an energy density of 5000 J/m^2 have also been plotted. There is much more difference between the defect and sound area in simulations as compared to experiments which can be attributed to 2D heat simulation instead of 3D heat conduction. There is a large separation in time between the defect and sound material, while in the experiments this is not the case, due to lateral heat transport that has not been modelled.

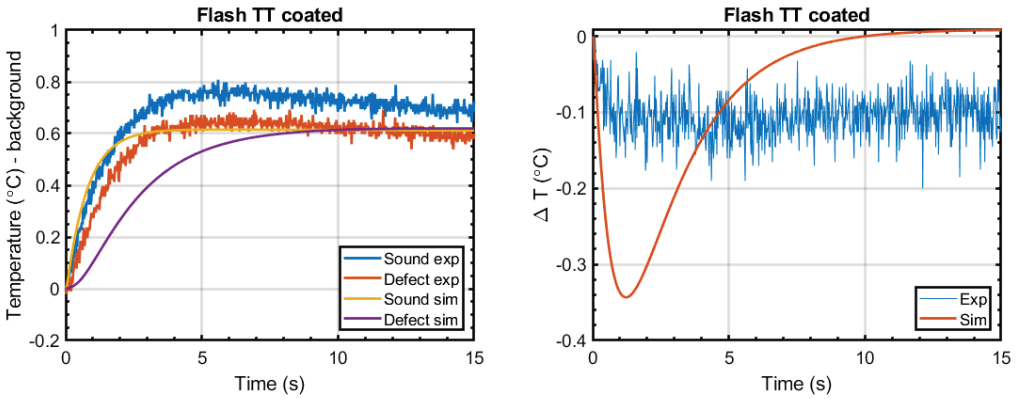

Figure 10: Flash TT experiment with increased ε and simulation. (left) Temperature vs time with a background subtraction. (Right) ΔT between defect and sound material as a function of time.

Another approach is to use the frequency domain to extract more data. Figure 11 shows phase images at 0.5 Hz of the panel containing a debond for the different ε values. In the uncoated case (ε≈0.16) the image is really noisy and it is difficult to detect the defect. By coating the sample with developer (ε≈0.30) results improve, but the image is still noisy. By pushing the camera to it most sensitive settings results are improved, as seen in the third figure.

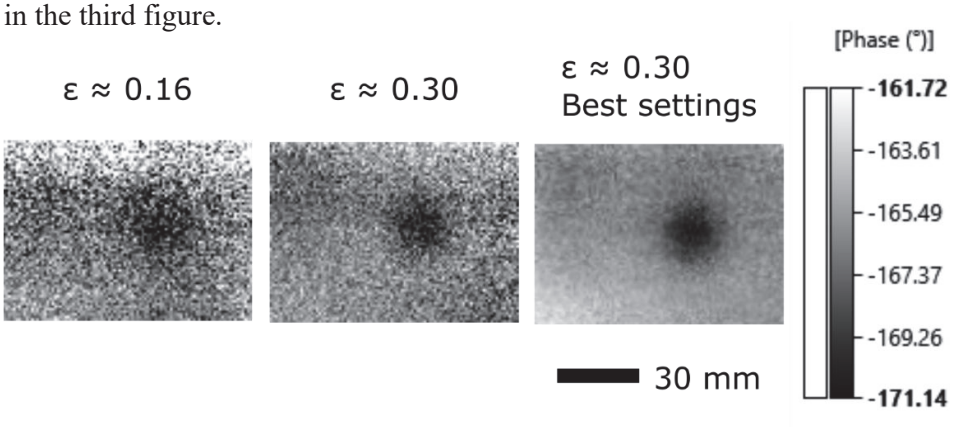

Figure 11: Phase images of the Flash TT experiments at 0.5 Hz.

However, the area under investigation is only 188x188 mm. The flash lamp was also positioned farther away such that the entire panel is illuminated, resulting in a power density of roughly 25 kJ/m^2. This power density proved to be too low to detect the debond anymore. Inserts, and porosity could not be detected using flash.

LPT

From the simulations, LPT showed the most temperature difference between defect and sound material. However, due to the dimensions of the lamps and illumination profile it was not possible to do a SS LPT measurement, since this would result in very low power densities. For the TT LPT experimental results showed that the total temperature increase

is only 0.2 to 0.5 °C. Correcting for emissivity these values are 1.2 to 3.1 °C meaning that the power densities are too low to be able to detect anything.

Lock-in thermography

Lock-in thermography has also been applied to the samples. SS inspection was not performed because the frequencies needed to detect defects are too high in practise. TT measurements were done on non-coated, coated samples and painted samples. For the non-coated samples the amplitude was very low (even when putting the halogen lamps close to the surface) resulting in no detectability of a defect. By applying developer on the surface results improve, but it is still impossible to see a defect. Instead of coating the samples with developer a thin layer (~~20~~ µm) of black matte paint was applied to both sides of the panel. This increased the emissivity from 0.16 to 0.9, allowing for a proper measurement of temperature and a lot of absorption of the light from the excitation lamps. Figure 12 shows the results of a lock-in inspection at 0.1 Hz for the different emissivity of samples considered.

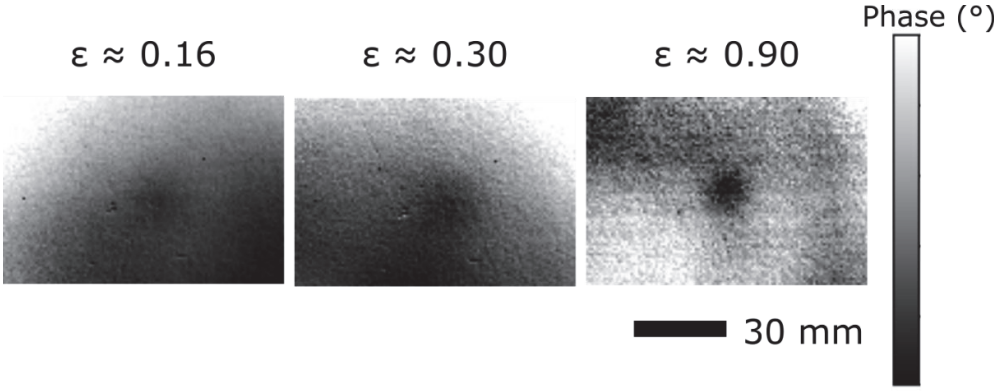

Figure 12: Phase images for a lock-in inspection at 0.1 Hz, with different emissivity's. Individual pictures have been scaled individually so numbers next to the scalebar are omitted.

For the lock-in inspections, samples coated with black matte paint showed defects.
From the panel containing the debond the amplitude and $\Delta\phi$ as a function of frequency can be determined, results are shown in Figure 13.

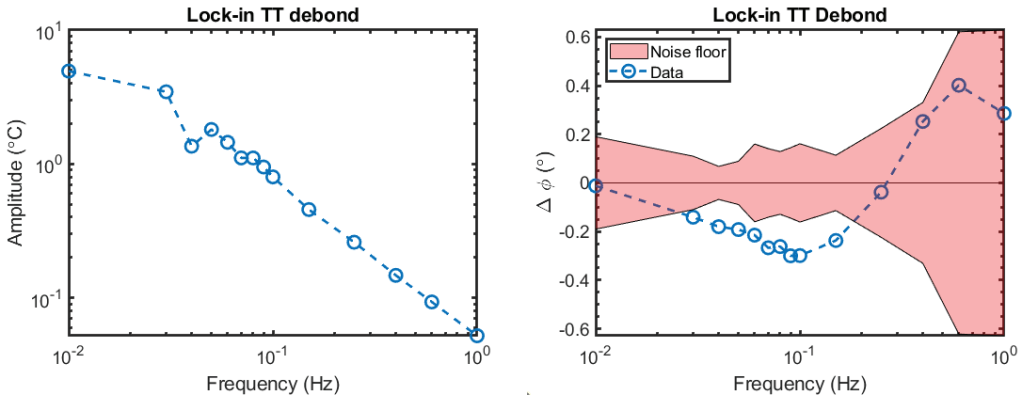

Figure 13: Results from experiments lock-in TT. (left) Amplitude as a function of frequency. (right) Δϕ as a function of frequency.

Amplitude values are still quite low, but it is possible to get phase values from the signal. The Δϕ vs frequency plot shows that around 0.1 Hz the maximum contrast is achieved, just as in the case with the simulations. However, the absolute phase value in simulations is around -26 °, while for the experiments this is only -0.3 °. This is just above the noise floor during experiment. The discrepancy between the simulation and experiment can be contributed to the fact that heat transport is only modelled in two directions instead of three. Nevertheless, the simulations correctly simulate the frequency at which Δϕ shows the most contrast.

Lock-in TT inspections were done on all samples shown in the reference sample section. Figure 14 shows the phase images of the insert, contamination and porosity panel at an inspection frequency of 0.1 Hz for the painted samples with an emissivity of 0.9. For the insert panel, the smaller 3x3 and 6x6 mm^2 could not reliably be detected. For the contamination panel, the debond could be detected as well as additional features which might correspond to the contaminations that have been put between the metal sheets. For the porosity panel, the porosity can be seen in the top section of the panel, as well as the metal shims that have been used.

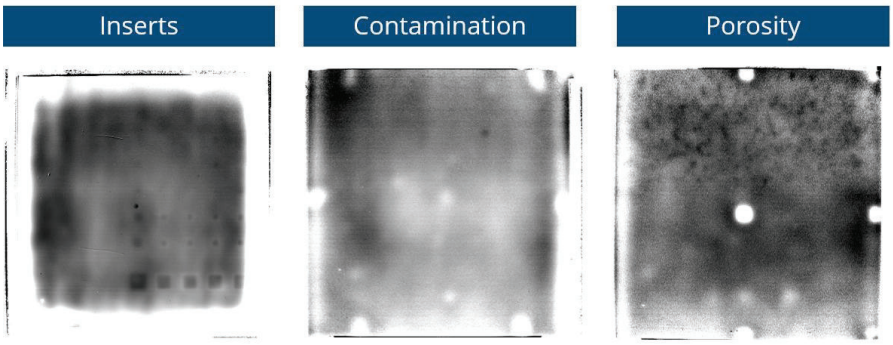

Figure 14: Lock-in TT inspection results at 0.10 Hz for all the panels considered in this study. Note that these results are after painting the samples.

Conclusions

Simulations using Civa have been performed to check the feasibility of using thermography to find defects within the adhesive layer of two 1.6 mm adhesively bonded sheets. Flash, long pulsed and lock-in thermography in both single sided and through transmission were simulated. For flash, high energy densities are needed to get a difference in temperature to see the effects of a defect. For LPT, higher temperature differences can be achieved due to longer heating times as compared to flash. For lock-in inspections, the difference in phase, $\Delta\phi$, is independent of the amplitude giving a single $\Delta\phi$ vs frequency curve. For SS inspections high frequencies are needed to see the defect, while this reduces for TT inspections. Experimental results for flash and lock-in thermography are given, showing that it is difficult to detect defects due to the low emissivity of the samples. By increasing emissivity, by coating or painting the samples, results improve. Absolute values between simulations do not agree well with experiments due to the way heat transport is modelled in the simulations. Nevertheless, simulations gave a good insight in the parameters that are essential. Especially, the frequency at which the contrast is the highest is correctly simulated. Lock-in TT experiments on reference panels showed that it is possible to detect inserts, debonds and porosity in adhesively bonded metallic structures as long as the emissivity of the sample is high.

Acknowledgements

The authors would like to thank GKN Fokker aerospace for suppling the reference panels and fruitful discussions.

Funding

This research was funded by the Dutch Ministry of Economic affairs, Rijksdienst voor ondernemend Nederland (RVO), grant number TSH21005, Advanced-alloy Sustainable Structures Enabling Technologies (ASSET).

Reference

1. Jansen, H.P.; van Elburg, B.; van Veen, E.S.; Platenkamp, D.J. Ultrasonic Frequency Analysis of Adhesively Bonded Joints. *Eng. Proc.* 2025, *90*, 20. https://doi.org/10.3390/engproc2025090020